Evaluation of ^{11}C-BU99008, a PET Ligand for the Imidazoline$_2$ Binding Sites in Rhesus Brain

Christine A. Parker*[1,2], Nabeel Nabulsi*[3], Daniel Holden[3], Shu-fei Lin[3], Tara Cass[3], David Labaree[3], Steven Kealey[4], Antony D. Gee[5], Stephen M. Husbands[6], Darren Quelch[1], Richard E. Carson[3], David J. Nutt[1], Yiyun Huang[3], and Robin J. Tyacke[1]

[1]*Centre for Neuropsychopharmacology, Hammersmith Hospital, Imperial College London, United Kingdom;* [2]*GSK, Global Imaging Unit, Stevenage, United Kingdom;* [3]*PET Center, Department of Diagnostic Radiology, Yale University, New Haven, Connecticut;* [4]*Institute of Psychiatry, De Crespigny Park, King's College London, London, United Kingdom;* [5]*Division of Imaging Sciences and Biomedical Engineering, King's College London, St Thomas' Hospital, London, United Kingdom; and* [6]*Department of Pharmacy and Pharmacology, University of Bath, Bath, United Kingdom*

The development of a PET radioligand selective for I_2-imidazoline binding sites (I_2BS) would enable, for the first time, specific, measurable in vivo imaging of this target protein, along with assessment of alterations in expression patterns of this protein in disease pathophysiology. **Methods:** BU99008 was identified as the most promising I_2BS radioligand candidate and radiolabeled with ^{11}C via methylation. The in vivo binding properties of ^{11}C-BU99008 were assessed in rhesus monkeys to determine brain penetration, brain distribution, binding specificity and selectivity (via the use of the unlabeled blockers), and the most appropriate kinetic model for analyzing data generated with this PET radioligand. **Results:** ^{11}C-BU99008 was demonstrated to readily enter the brain, resulting in a heterogeneous distribution (globus pallidus > cortical regions > cerebellum) consistent with the reported regional I_2BS densities as determined by human tissue section autoradiography and preclinical in vivo PET studies in the pig. In vivo competition studies revealed that ^{11}C-BU99008 displayed reversible kinetics specific for the I_2BS. The multilinear analysis (MA1) model was the most appropriate analysis method for this PET radioligand in this species. The selective I_2BS blocker BU224 was shown to cause a saturable, dose-dependent decrease in ^{11}C-BU99008 binding in all regions of the brain assessed, further demonstrating the heterogeneous distribution of I_2BS protein in the rhesus brain and binding specificity for this radioligand. **Conclusion:** These data demonstrate that ^{11}C-BU99008 represents a specific and selective PET radioligand for imaging and quantifying the I_2BS, in vivo, in the rhesus monkey. Further work is under way to translate the use of ^{11}C-BU99008 to the clinic.

Key Words: imidazoline$_2$ binding site; I_2BS; positron emission tomography; PET; BU99008

J Nucl Med 2014; 55:838–844
DOI: 10.2967/jnumed.113.131854

The ability of the α_2-adrenoceptor agonist clonidine and the antagonist idazoxan to label a subpopulation of binding sites, not displaceable by the endogenous ligand noradrenaline, led to the discovery of the imidazoline binding sites some 20 y ago. These binding sites have subsequently been divided into 3 groups: the imidazoline$_1$ binding site, which is preferentially labeled by ^{3}H-clonidine; the imidazoline$_2$ binding site (I_2BS), which is preferentially labeled by ^{3}H-idazoxan; and the imidazoline$_3$ binding site, which is an atypical imidazoline site found on pancreatic β-cells (*1*).

I_2BS are known to reside on the mitochondrial membranes of astrocytes (*2*). Changes in postmortem binding density of the I_2BS have implicated them in a range of psychiatric conditions such as depression and addiction, along with neurodegenerative disorders such as Alzheimer disease and Huntington chorea (*3*). Functional interactions in preclinical models have also been shown in relation to the opioid system, in which I_2BS ligands have been shown to affect tolerance to morphine (*4*) and alleviate some of the morphine withdrawal syndrome in rats (*5*). I_2BS ligands have also been shown acutely to affect feeding and appetite by an as-yet undetermined mechanism (*6*). The location of I_2BS on glial cells and the possibility that they may in some way regulate glial fibrillary acidic protein (*7*) have led to increased interest into the role of I_2BS and I_2BS ligands in conditions characterized by marked gliosis. The density of I_2BS has been shown to increase in Alzheimer disease postmortem (*3*), and it has also been suggested that I_2BS may be a marker for human glioblastomas (*8*). Subsequent publications added weight to this argument, showing that the density of I_2BS is increased in vivo with heat-induced gliosis (*9*). Additionally, Callado et al. have shown not only an increase in the I_2BS in human gliomas but also that this increase in binding sites was correlated with the severity and malignancy of the glioma (*10*).

PET is an in vivo imaging technique that uses radioligands as selective molecular probes to map the location and density of specific proteins. The development of a selective I_2BS PET radioligand would allow for the characterization of I_2BS in vivo and its regulation in disease states. Several ligands selective for I_2BS have been reported, but only 2 potential PET radioligands have been reported to date: the radiosynthesis of ^{11}C-benazoline, but its study in vivo has not been reported (*11*), and the radiosynthesis and in vivo imaging evaluation of ^{11}C-2-(3-fluoro-4-^{11}C-tolyl)-4,5-dihydro-1H-imidazole in nonhuman primates (*12*), although the specific binding signal appears to be low for this radioligand.

We have recently reported the synthesis, in vitro and in vivo evaluation, and radiosynthesis of a PET radioligand for the I_2BS, ^{11}C-BU99008 (*13,14*). In this article, we report the preclinical in

Received Sep. 5, 2013; revision accepted Jan. 24, 2014.
For correspondence or reprints contact: Robin J. Tyacke, Centre for Neuropsychopharmacology, Imperial College London, Burlington Danes Building, Hammersmith Hospital, 160 Du Cane Rd., London W12 0NN, United Kingdom.
E-mail: r.tyacke@imperial.ac.uk
*Contributed equally to this work.
Published online Apr. 7, 2014.

vivo evaluation of ^{11}C-BU99008, for imaging I_2BS, in the rhesus monkey brain.

MATERIALS AND METHODS

Chemicals

^{3}H-BU99008 (specific activity, 1.04 TBq/mmol) was custom synthesized by Sibtech. Challenge drugs moclobemide and lazabemide were obtained from commercial suppliers: Sigma-Aldrich Co. Ltd. and Tocris Biosciences. Dr. Stephen Husbands synthesized the BU224. All other chemicals and reagents were purchased from commercial suppliers and used without further purification.

Animals

All animal experiments were performed in accordance with the U.K. Animals (Scientific Procedures) Act 1986. PET imaging experiments in rhesus monkeys were conducted in accordance with a protocol approved by the Yale University Institutional Animal Care and Use Committee.

In Vitro Competition Binding Studies

Membrane preparation, competition binding studies, and data analysis were conducted as previously described (*13*) with the following alterations. Rat (male; Wistar; weight, 250–300 g) and Cynomolgus monkey brains were used and resulting membrane preparations stored at −80°C. The displacement binding studies for the ^{3}H-BU99008 (1 nM) were conducted at 37°C in assay buffer (50 mM Tris-HCl, 140 mM NaCl, 1.5 mM $MgCl_2$, 5 mM KCl, 1.5 mM $CaCl_2$, pH7.4), and radioactivity was determined using a Tricarb 2900 β-counter (PerkinElmer). Protein content was determined using a Pierce bicinchoninic acid kit.

PET Imaging Studies in Rhesus Monkeys (*Macaca mulatta*)

Radiochemistry. ^{11}C-BU99008 was prepared by *N*-alkylation of the desmethyl precursor BU99007 with ^{11}C-CH_3I in the AutoLoop synthesis module (Bioscan). A description of the synthetic methods can be found in the supplemental information (Supplemental Fig. 1; available at http://jnm.snmjournals.org).

Study Design. Two Rhesus monkeys (female; weight, ~6 and ~7 kg; age, 7 and 8 y) were used, with scanning days at least 14 d apart. Each animal had 5 scanning days. Each scanning day consisted of a baseline scan with ^{11}C-BU99008 (120 min); after this, animals received an intravenous injection of blocking drug over a 10-min period, approximately 10 min before initiation of a second scan with ^{11}C-BU99008 (120 min), to determine binding specificity and selectivity of the radioligand (Supplemental Table 1). The administration of the specific I_2BS ligand, BU224, was 0.01, 0.03, and 0.3 mg/kg for monkey 1 and 0.01, 0.03, and 0.1 mg/kg for monkey 2. To assess the selectivity of binding to I_2BS, both animals received an injection of the reversible monoamine oxidase A (MAO_A) inhibitor moclobemide (1 mg/kg) and the reversible MAO_B inhibitor lazabemide (0.5 mg/kg). Data acquisition started simultaneously with ligand injection. Vital signs were monitored at least 4 times per hour and more frequently after injection of tracer and blocking drugs.

MR Imaging. Images were acquired for each monkey on a 3.0-T Trio scanner (Siemens), using an extremity coil. T_1-weighted images were acquired in the coronal plane with a spin-echo sequence (echo time, 3.34; repetition time, 2,530; flip angle, 7°; section thickness, 0.50 mm; field of view, 140 mm; image matrix, 256 × 256 × 176 pixels; matrix size, 0.547 × 0.547 × 0.500 mm). The whole-brain image was cropped to 176 × 176 × 176 pixels using MEDx software (Medical Numerics) before coregistration with PET image data.

PET Imaging Procedures. Animals were sedated with an intramuscular injection of ketamine hydrochloride (10 ± 2 mg/kg), approximately 2 h before the start of scanning, transported to the PET facility, anesthetized using isoflurane, intubated, and maintained on oxygen and 1.5%–2.5% isoflurane throughout the study. PET scans were obtained on the Focus 220 PET scanner (Siemens Preclinical Solutions), with a reconstructed image resolution of approximately 1.5 mm. After a transmission scan, 170 ± 14 MBq (4.6 ± 0.4 mCi; mass dose, 0.08 ± 0.02 μg/kg) of ^{11}C-BU99008 was injected over 3 min. List-mode data were acquired for 120 min and binned into sinograms with the following frame timing: 6 × 30 s, 3 × 1 min, 2 × 2 min, and 22 × 5 min. Dynamic scan data were reconstructed with a filtered-backprojection algorithm with corrections for attenuation, normalization, scatter, and randoms.

Arterial Blood Sampling. Arterial blood samples were collected for the determination of whole blood and plasma input functions and metabolite analysis and plasma-free fraction of ^{11}C-BU99008. These procedures are described in detail in the supplemental information.

Regional Time–Activity Curve Computation. An existing region-of-interest (ROI) map defined on a template brain (a representative MR image of a rhesus brain) was used. The following, a priori defined, ROIs were examined: cingulate, frontal, insula, and occipital cortex; brain stem; pons; cerebellum; caudate; putamen; globus pallidus; and thalamus. A nonlinear transformation was estimated using the Bioimagesuite software (http://www.bioimagesuite.org/) to transfer the ROI template to the MR image of each animal used during this study. These regions were then transferred to the PET images based on a rigid transformation matrix (*15*) and used to generate time–radioactivity curves (time–activity curve).

Kinetic Modeling. Regional time–activity curves were analyzed using 1- and 2-tissue-compartment models (1TC and 2TC) and multilinear analysis (MA1) (*16*) to calculate regional distribution volume (V_T). MA1 is a linear method related to Logan analysis but with less noise-induced bias. Like Logan analysis, data are fitted starting at a specified time, t^*; here t^* is 20 min. The optimal model was based on quality of fit and the uncertainty (SE) of the V_T parameter estimate. For blocking studies, because there was no suitable reference region, a graphical method was used to calculate the nondisplaceable volume of distribution (V_{ND}) and global receptor occupancy (*17*).

To derive the blocking dose needed to induce 50% global and regional receptor occupancy (ED_{50}), the 3-parameter dose–response curve was used (GraphPad Prism, version 6.0 d for Mac OS X; GraphPad Software [www.graphpad.com]). For the global ED_{50}, the occupancy calculated from Cunningham et al. (*17*), which accounts for V_{ND}, was used. For regional ED_{50}, the percentage reduction in V_T values from baseline after various blocking doses of drug, which does not account for V_{ND}, were calculated and fitted to this equation.

RESULTS

In Vitro Competition Binding Studies

^{3}H-BU99008 in vitro competition data demonstrated a 2-site fit to the rodent brain with BU224, exhibiting a half maximal inhibitory concentration for the high-affinity site value of 50.5 ± 12.9 nM (Table 1), consistent with previous data (*13*). In contrast, competition of BU224 in cynomolgus brain yielded a single-site fit, with a half maximal inhibitory concentration value of 130.2 ± 33.9 nM (Table 1). The competition of ^{3}H-BU99008 from both rat and cynomolgus brains by the MAO_B inhibitor lazabemide exhibited poor inhibition of binding, and the MAO_A inhibitor moclobemide showed no inhibition at the highest concentration used (Table 1).

Radiochemistry

Injection-ready ^{11}C-BU99008 was successfully synthesized with a chemical yield of 32% ± 17% (decay-corrected), radiochemical purity of greater than 99%, and a specific activity of 146 ± 33 MBq/nmol (3.95 ± 0.90 mCi/nmol, n = 19) at the end of synthesis. The identity of the radiolabeled product was confirmed by coinjection with a sample of authentic BU99008, which, under the same elution conditions, showed an identical retention time.

TABLE 1
In Vitro I_2BS Binding Affinities of Blocking Drugs in Rat and Nonhuman Primate Brain Using ^{3}H-BU99008

Protein target	Blocking drug	IC_{50} ± SD (nM)	
		Rat	Cynomolgus
I_2BS	BU224	50.5 ± 12.9 (high) 9,596 ± 2,494 (low)	130.2 ± 33.9
MAO_A	Moclobemide	>100,000	>100,000
MAO_B	Lazabemide	6,445 ± 1,733	17,370 ± 2,068

Displacement of ^{3}H-BU99008 by BU224 was best fit to 2-site model in rat only; for all other instances data were best fit to 1-site model (n = 4).

IC_{50} = half maximal inhibitory concentration.

In Vivo Blood Data

Free fraction of ^{11}C-BU99008 in the plasma was high, at 0.68 ± 0.07 (n = 19). The amount of total radioactivity measured in plasma was similar between baseline scans and after administration of either the MAO inhibitors or the I_2BS inhibitor (Fig. 1A). In addition, radio–high-performance liquid chromatography analysis revealed ^{11}C-BU99008, under baseline conditions, to be rapidly metabolized in plasma, with the parent compound representing about 50% of the total radioactivity 20 min after administration (Fig. 1B). However, there was a small decrease in the parent fraction of ^{11}C-BU99008 after administration of all 3 inhibitors, compared with data acquired under baseline conditions, for which the parent compound represented about 50% of the total radioactivity at 15 min after administration (Fig. 1B).

In Vivo PET Studies

Representative baseline PET images and corresponding time–activity curves for ^{11}C-BU99008 uptake into the rhesus brain are given in Figures 2B and 3A, respectively. ^{11}C-BU99008 readily entered the brain, with the highest uptake observed in the globus pallidus, caudate, and thalamus; with moderate uptake in the cortical and putamen regions; and with lowest uptake in the cerebellum and occipital cortex. Peak radioactivity concentrations were observed approximately 15–25 min after administration of ^{11}C-BU99008, followed by a slow washout from all regions (Fig. 3A).

The regional time–activity curves were analyzed by the reversible 1TC and 2TC models and by the MA1 model (*16*). The 2TC model produced good fits to the data, but more than 20% of fits to baseline data had unreliable V_T estimates—that is, a percentage SE (%SE) greater than 20%. Poor reliability occurred most often in smaller, noisier regions and in baseline scans or scans with little effective blockade (see below). The 1TC model showed clear lack of fit in most cases. Also, the V_T values from the 1TC underestimated those from the 2TC by 10%–40% (excluding 2TC values with high %SE), with the relationship of $V_{T(1T)} = 0.87 \times V_{T(2T)} - 4.2$, $r^2 = 0.92$. The MA1 method produced good fits and stable estimates for V_T, with small differences in V_T values using different t* values from 20 to 40 min. In the cases in which 2TC values had a %SE less than 20%, the relationship between MA1 and 2TC values was $V_{T(MA1)} = 0.94 \times V_{T(2T)} - 1.3$, $r^2 = 0.97$. On the basis of the bias from 1TC fits, and the numerous cases of high %SE from 2TC, MA1 with a t* of 20 min was chosen for derivation analysis.

Table 2 lists MA1-derived regional V_T values from individual baseline scans. The baseline data acquired from the 2 rhesus monkeys were demonstrated to be reproducible and consistent throughout the course of the study (Fig. 4). When the MA1 model with a t* of 20 min was used, baseline V_T values were highest in the globus pallidus (114.2 ± 24.0 mL/cm), caudate (109.7 ± 13.7 mL/cm), and thalamus (96.3 ± 8.1 mL/cm) and lowest in the cerebellum (48.1 ± 4.8 mL/cm). This rank order of regional V_T for ^{11}C-BU99008 from the baseline data (globus pallidus > cortex > cerebellum, Table 2) is consistent with reported I_2BS densities and distribution determined by tissue-section autoradiography in humans (*18*) and in vivo pig PET (*14*). Furthermore, the mean rhesus V_T values were significantly correlated ($r^2 = 0.72$; $P < 0.05$) with the mean V_T values from our previous in vivo porcine ^{11}C-BU99008 PET data (inset, Fig. 4) ((*14*); S. Kealey, E.M. Turner, S.M. Husbands, et al., unpublished data, 2013, from the porcine study).

In vivo blocking studies using the MAO_A and MAO_B inhibitors moclobemide and lazabemide, respectively, did not cause any significant change in binding signal of ^{11}C-BU99008 to any regions studied (Figs. 2C and 2E; Supplemental Fig. 2). In vivo competition using ^{11}C-BU99008 plus increasing doses of the selective I_2BS blocker, BU224, yielded a dose-dependent decrease in uptake of ^{11}C-BU99008 in all regions studied. The highest dose administered (0.3 mg/kg) yielded an apparent near-to-full blockade, suggesting high selectivity of this radioligand for the I_2BS (Figs. 2G, 3B, and 5; Table 3). The presence of a dose-dependent decrease in binding in the cerebellum suggests this is not a suitable reference region for analysis of ^{11}C-BU99008.

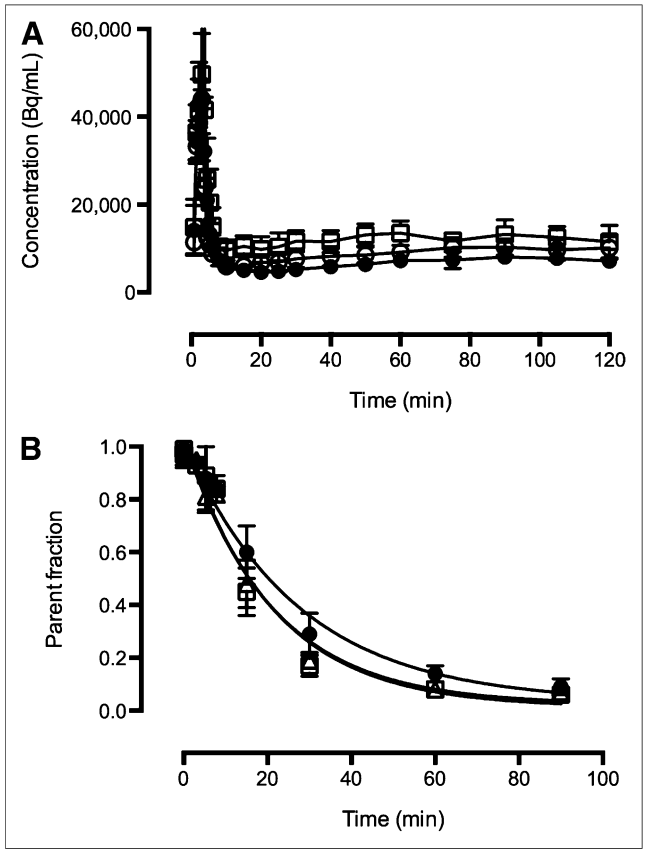

FIGURE 1. Mean total plasma radioactivity (A) and metabolite data (B) for ^{11}C-BU99008 scan. ● = baseline scan data; △ = blocking scan data using MAO inhibitors; □ = blocking scan data using BU224. Each point represents mean of all scans in that group; vertical bars represent SD.

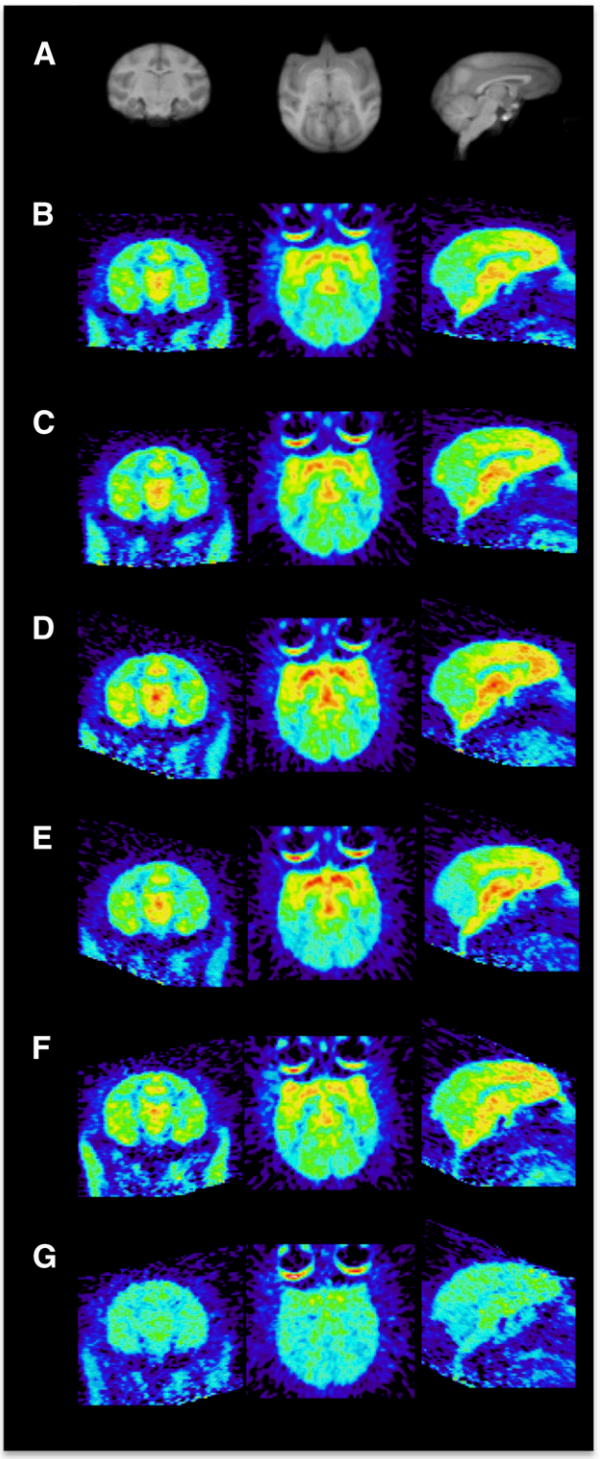

FIGURE 2. Representative coronal, transverse, and sagittal images of ^{11}C-BU99008 uptake in rhesus brain. Images are summed from 30 to 45 min after radioligand injection and displayed as SUVs. (A) Structural MR imaging. (B and C) Baseline (B) and moclobemide preblock (C) (1 mg/kg). (D and E) Baseline (D) and lazabemide preblock (E) (0.5 mg/kg). (F and G) Baseline (F) and BU224 preblock (G) (0.3 mg/kg). Paired scans B and C, D and E, and F and G were obtained on same day.

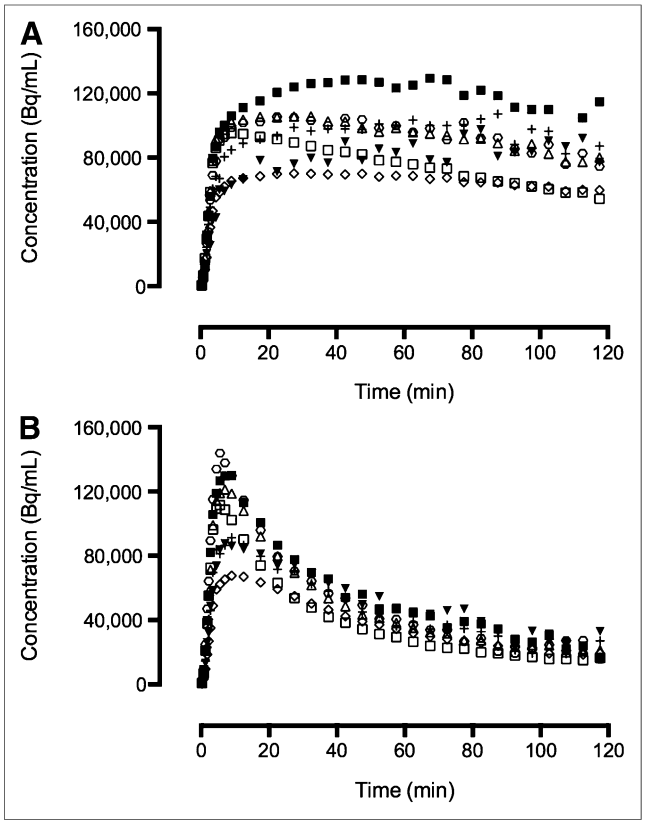

FIGURE 3. Representative time–activity curves for ^{11}C-BU99008 in selected ROIs in rhesus brain. (A) Baseline ^{11}C-BU99008 scan. (B) ^{11}C-BU99008 scan after administration of BU224 (0.3 mg/kg). ■ = caudate; □ = cerebellum; △ = frontal cortex; ▼ = globus pallidus; ◇ = occipital cortex; ○ = putamen; + = thalamus.

A global receptor occupancy measure was calculated for the BU224 studies using the occupancy plot (*17*). Occupancy values ranged from 25% to 35% for the lowest dose of BU224 (0.01 mg/kg) to 93% for the highest dose (0.3 mg/kg). These occupancies were plotted versus administered dose (d) in Figure 6, with a fit to the equation $\text{Occ} = d/(d + ED_{50})$, which yielded an ED_{50} estimate of 0.022 mg/kg for the whole brain (Table 3).

TABLE 2
Baseline Regional V_T Values (mL/cm) for ^{11}C-BU99008 Using MA1

Brain region	MA1 V_T (mean ± SD)
Globus pallidus	114.2 ± 24.0
Caudate	109.7 ± 13.7
Thalamus	96.3 ± 8.1
Putamen	75.7 ± 7.8
Frontal cortex	75.1 ± 14.2
Cingulate cortex	85.5 ± 13.0
Occipital cortex	50.5 ± 7.3
Insula cortex	76.3 ± 9.2
Pons	70.1 ± 6.9
Brain stem	75.2 ± 8.5
Cerebellum	48.1 ± 4.8

Values are computed with t* = 20 min (n = 8).

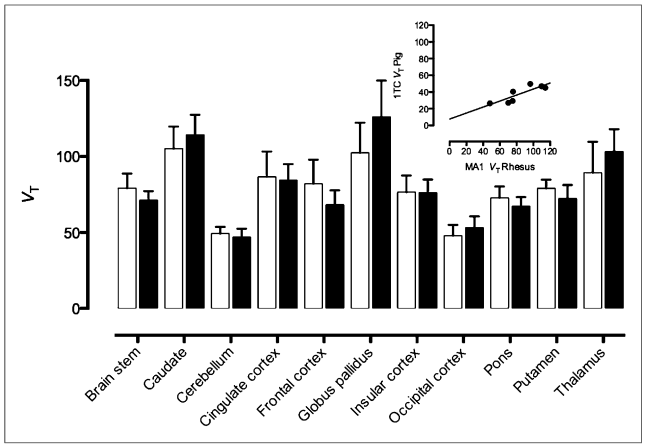

FIGURE 4. Bar chart showing regional distribution volume (V_T) of ^{11}C-BU99008 from 2 animals (monkey 2, open bars, and monkey 1, filled bars). These represent mean ± SD from 4 separate baseline scans. Insert shows significant correlation ($r^2 = 0.72$; $P < 0.05$) between mean V_T from this study (both animals) and porcine study ($n = 3$) ((*14*); S. Kealey, E.M. Turner, S.M. Husbands, et al., unpublished data, 2013, data from porcine study). Regional V_T values were generated using MA1 model (t* = 20 min) for rhesus data and 1TC model for porcine data.

Regional ED_{50} values for BU224 were also calculated for the globus pallidus, frontal cortex, and cerebellum using the percentage reduction in V_T instead of the estimated global occupancy value (Supplemental Figs. 3A–3C). Calculated regional ED_{50} values were 0.017 mg/kg for the globus pallidus, 0.017 mg/kg for the frontal cortex, and 0.016 mg/kg for the cerebellum (Supplemental Fig. 3; Table 3).

DISCUSSION

This paper describes the radiosynthesis of ^{11}C-BU99008 and its characterization as a novel PET radioligand for the quantification of central I_2BS in vivo in rhesus monkeys.

BU99008 was selected as the most suitable compound for radiolabeling with a PET radioisotope for imaging the I_2BS, as reported previously by our group (*13*). In addition, BU99008 exhibited selectivity and nanomolar affinity for the I_2BS in the rodent and cynomolgus brain (Table 1). Interestingly, a 2-site model fit was preferred for the rodent and a 1-site fit for the cynomolgus brain tissue, suggesting that, in the rodent brain, BU99008 exhibits a degree of affinity for a second binding site, which may be unrelated to the I_2BS, possibly reflecting a MAO binding component (*19*). Importantly, because of the nature of the I_2BS being colocalized with MAOs on the outer membrane mitochondrial enzymes (*20*), it was essential to investigate the relative affinities of selective MAO_A and MAO_B inhibitors for the I_2BS to proceed. In vitro studies using cynomolgus brain demonstrated MAO inhibitors to possess a low affinity for the I_2BS in (Table 1). However, in the rodent brain tissue, the MAO_B inhibitor possessed a similar affinity for the low-affinity binding site exhibited previously in the rodent brain by BU224 (Table 1). These data confirm the notion that the high-affinity binding component, in vitro, in both the rat and the cynomolgus brain is expected to represent the I_2BS.

In view of these in vitro data, and combined with a successful radiolabeling feasibility assessment, we progressed the development of BU99008 as a PET ligand via evaluation in porcine brain, in vivo (*14*). In that study, ^{11}C-BU99008 demonstrated reversible kinetics and a brain distribution consistent with the known binding site densities and localization for the I_2BS protein and a dose-dependent decrease in V_T after administration of the selective I_2BS blocker BU224. Further studies in pigs showed a small, but relevant, binding component associated with MAO (R.J. Tyacke, S. Kealey, J. Myers, et al., unpublished data, 2013). Therefore, given that relative expression levels of I_2BS and MAO differs from species to species, to progress ^{11}C-BU99008 for use in human studies we decided to assess this PET ligand further, preclinically, in rhesus monkeys, because we predict human brain uptake and in vivo binding characteristics of this particular PET ligand would be more similar to rhesus brain than porcine brain. BU99008 was successfully radiolabeled with ^{11}C with good reproducibility, radiochemical yields, and high specific activities.

After injection into a rhesus monkey, the radioligand ^{11}C-BU99008 metabolized fairly quickly, with only approximately 30% of the parent compound remaining at 30 min after injection. A slight acceleration in metabolism was also observed when blocking agents were given before ^{11}C-BU99008 injection, but this effect was modest and unlikely to affect the usability of this ligand.

In monkey brain, ^{11}C-BU99008 displayed differential regional uptake. This heterogeneous distribution of ^{11}C-BU99008 exhibited the following rank order: globus pallidus and other basal ganglia regions > cortex > cerebellum, consistent with the known I_2BS densities and results from human tissue–section autoradiography (*18*) and porcine PET imaging experiments (*14*). Although the cerebellum showed the lowest brain uptake, there was still a decrease in V_T values after BU224 blockade (Fig. 4), indicating the cerebellum would be unsuitable as a reference region. This was consistent with the findings of our previous study in pigs (*14*).

An assessment of the intrasubject variability was performed that yielded low to moderate variability in the V_T values obtained for each ROI studied for each subject across multiple baseline scans (Fig. 4). Furthermore, comparison of interspecies variability between the rhesus monkeys used in this study and pigs used previously by our group with this PET radioligand (*14*) demonstrated a significant correlation (inset, Fig. 4), suggesting a degree of correspondence between these 2 species for the I_2BS. ^{11}C-BU99008, however, appears to be affected by MAO inhibitors in the pig, which is a phenomenon not exhibited in the rhesus (R.J. Tyacke, S. Kealey, J. Myers, et al., unpublished data, 2013).

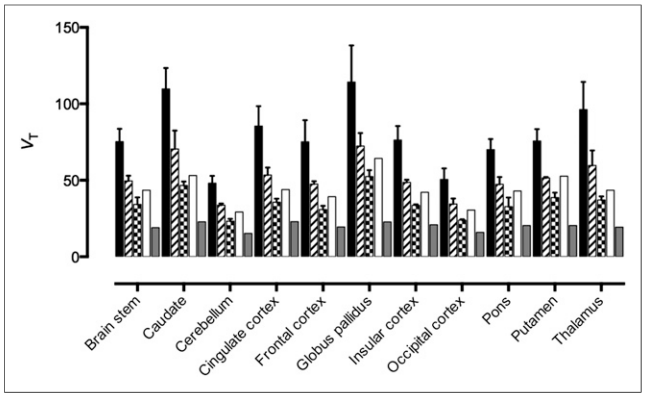

FIGURE 5. Bar chart showing regional distribution volume (V_T) of ^{11}C-BU99008 and effect of increasing doses of I_2BS ligand BU224: 0.01 mg/kg (striped), 0.03 mg/kg (checkered), 0.1 mg/kg (clear), 0.3 mg/kg (gray), and baseline (black). Bars represent mean ± SD; V_T generated using MA1 model.

TABLE 3
Calculated Fraction of I_2BS Occupied by BU224 Using ^{11}C-BU99008

BU224 dose (mg/kg)	Percentage occupancy							
	Whole brain		Globus pallidus		Frontal cortex		Cerebellum	
0.01	35 (1)	25 (2)	38 (1)	32 (2)	32 (1)	24 (2)	30 (1)	27 (2)
0.03	54 (1)*	66 (2)	50 (1)*	61 (2)	48 (1)*	65 (2)	47 (1)*	54 (2)
0.1	81 (2)		74 (2)		73 (2)		64 (2)	
0.3	93 (1)		85 (1)		75 (1)		72 (1)	
ED_{50}	0.022		0.017		0.017		0.016	

*Percentage occupancies generated from averaged composite of baseline scans for monkey 1 due to failure to obtain baseline scan on this study day.

Number in parentheses indicates animal used to derive value: monkey 1 (1) and monkey 2 (2). Whole-brain occupancy was calculated using occupancy plot (*17*) and is derived from slope for all reported brain regions. Values calculated from V_T determined using MA1 model.

The effects of the MAO_A inhibitor moclobemide and the MAO_B inhibitor lazabemide on ^{11}C-BU99008 binding were determined in vivo, in rhesus monkeys, and found to cause no significant decrease in V_T in any of the ROIs assessed (Supplemental Fig. 2). This key finding suggests that in rhesus monkey brain any contribution of the ^{11}C-BU99008 signal due to binding to MAO is small or negligible and would not be expected to cause any significant interference with the assessment of I_2BS binding signal in this species.

After administration of increasing blocking doses of BU224, a dose-dependent decrease in ^{11}C-BU99008 V_T was observed in all regions of the rhesus brain (Fig. 5), confirming the absence of a reference region for this PET radioligand and remaining consistent with the known distribution profile for I_2BS in the brain. The dose-dependent decrease in V_T observed for all ROIs studied is not thought to represent a global change unrelated to the specific binding of ^{11}C-BU99008 and the blocking by BU224 given that a heterogeneous signal was observed across the ROI under baseline conditions, differential levels of decrease in V_T values were observed for each region after increasing doses of BU224, and a plateau at a V_T value of approximately 20 mL/cm was achieved for all ROIs after the highest dose of BU224 administered (0.3 mg/kg; Fig. 5). Additionally, the dose-dependent blockade by the selective I_2BS inhibitor in the rhesus brain confirmed the specificity of ^{11}C-BU99008 for the I_2BS and demonstrated a blockade of approximately 90% across all ROIs at the highest dose administered (0.3 mg/kg). Interestingly, the in vivo ED_{50} of BU224 generated across all brain regions was consistent with the presence of 1 binding site and generated a value of 0.022 mg/kg (Fig. 6), which is consistent with the known in vitro and ex vivo properties of this compound (*5*).

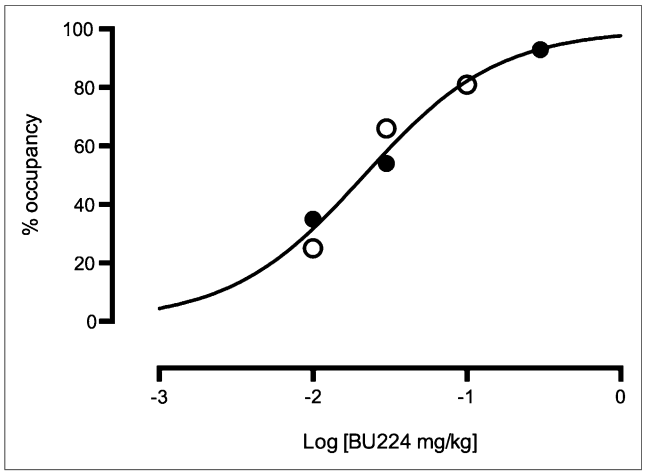

FIGURE 6. Dose-dependent occupancy by BU224 in whole brain; occupancy calculated using occupancy plot (ED_{50} = 0.022 mg/kg) (*17*). V_T data generated using MA1 model. ● = monkey 1; ○ = monkey 2.

Given these data, we predict that ^{11}C-BU99008 should demonstrate a binding distribution profile in the human brain similar to that observed from this study in the rhesus monkey, in which the rank order of regional brain uptake for this ligand would be expected to be globus pallidus > cortical regions > cerebellum. For modeling purposes, because MA1 consistently produced good fits to the data along with reliable and stable estimates of V_T for all regions of the rhesus brain studied, the use of this particular model for analysis of PET data generated using ^{11}C-BU99008 should be considered in future studies. Work is under way to assess the utility of ^{11}C-BU99008 as a PET ligand for in vivo imaging and quantification of I_2BS in the human population, and if deemed useful, its applicability for determining alterations in I_2BS density and distribution in known disease states will be investigated.

CONCLUSION

This article reports the radiolabeling and pharmacologic investigation of ^{11}C-BU99008 as a novel I_2BS PET radioligand in rhesus monkeys. In vivo distribution of ^{11}C-BU99008 in the rhesus monkey brain demonstrated the following rank order of regional uptake: globus pallidus > cortex > cerebellum, consistent with the known distribution profile of the I_2BS. ^{11}C-BU99008 displayed reversible kinetics and specificity for the I_2BS, with the MA1 model representing the most appropriate analysis method for the derivation of binding parameters for this PET radioligand. The data reported here provide evidence for ^{11}C-BU99008 to represent a potentially useful PET imaging tool for probing the I_2BS. Work is under way to progress ^{11}C-BU99008 for assessment of its clinical utility as a PET radioligand for I_2BS.

DISCLOSURE

The costs of publication of this article were defrayed in part by the payment of page charges. Therefore, and solely to indicate this fact, this article is hereby marked "advertisement" in accordance

with 18 USC section 1734. This study was funded by the MRC (G0801501) and GSK. No other potential conflict of interest relevant to this article was reported.

ACKNOWLEDGMENTS

We thank Roger Gunn and Eugenii Rabiner for interesting discussions and their continued support of this study.

REFERENCES

1. Eglen RM, Hudson AL, Kendall DA, et al. 'Seeing through a glass darkly': casting light on imidazoline 'I' sites. *Trends Pharmacol Sci.* 1998;19:381–390.
2. Regunathan S, Feinstein DL, Reis DJ. Expression of non-adrenergic imidazoline sites in rat cerebral cortical astrocytes. *J Neurosci Res.* 1993;34:681–688.
3. García-Sevilla JA, Escriba PV, Guimon J. Imidazoline receptors and human brain disorders. *Ann N Y Acad Sci.* 1999;881:392–409.
4. Ruiz-Durántez E, Torrecilla M, Pineda J, Ugedo L. Attenuation of acute and chronic effects of morphine by the imidazoline receptor ligand 2-(2-benzofuranyl)-2-imidazoline in rat locus coeruleus neurons. *Br J Pharmacol.* 2003;138:494–500.
5. Hudson AL, Gough R, Tyacke R, et al. Novel selective compounds for the investigation of imidazoline receptors. *Ann N Y Acad Sci.* 1999;881:81–91.
6. Hudson AL, Nutt DJ, Husbands SM. Imidazoline receptors and their role in depression. *Pharm News.* 2001;8:26–32.
7. Olmos G, Alemany R, Escriba PV, Garcia-Sevilla JA. The effects of chronic imidazoline drug treatment on glial fibrillary acidic protein concentrations in rat brain. *Br J Pharmacol.* 1994;111:997–1002.
8. Martín-Gómez JI, Ruiz J, Callado LF, et al. Increased density of I2-imidazoline receptors in human glioblastomas. *Neuroreport.* 1996;7:1393–1396.
9. Martín-Gómez JI, Ruiz J, Barrondo S, Callado LF, Meana JJ. Opposite changes in imidazoline I2 receptors and alpha2-adrenoceptors density in rat frontal cortex after induced gliosis. *Life Sci.* 2005;78:205–209.
10. Callado LF, Martin-Gomez JI, Ruiz J, Garibi JM, Meana JJ. Imidazoline I_2 receptor density increases with the malignancy of human gliomas. *J Neurol Neurosurg Psychiatry.* 2004;75:785–787.
11. Roeda D, Hinnen F, Dolle F. Radiosynthesis of a 2-substituted 4,5-dihydro-^{1}H-[2-C-11] imidazole: the I-2 imidazoline receptor ligand [Cl-11 benazoline. *J Labelled Compd Rad.* 2003;46:1141–1149.
12. Kawamura K, Maeda J, Hatori A, et al. In vivo and in vitro imaging of I_2 imidazoline receptors in the monkey brain. *Synapse.* 2011;65:452–455.
13. Tyacke RJ, Fisher A, Robinson ES, et al. Evaluation and initial in vitro and ex vivo characterization of the potential positron emission tomography ligand, BU99008 (2-(4,5-dihydro-^{1}H-imidazol-2-yl)-1- methyl-^{1}H-indole), for the imidazoline(2) binding site. *Synapse.* 2012;66:542–551.
14. Kealey S, Turner EM, Husbands SM, et al. Imaging imidazoline-I2 binding sites in porcine brain using ^{11}C-BU99008. *J Nucl Med.* 2013;54:139–144.
15. Sandiego CM, Weinzimmer D, Carson RE. Optimization of PET-MR registrations for nonhuman primates using mutual information measures: a multi-transform method (MTM). *Neuroimage.* 2013;64:571–581.
16. Ichise M, Toyama H, Innis RB, Carson RE. Strategies to improve neuroreceptor parameter estimation by linear regression analysis. *J Cereb Blood Flow Metab.* 2002;22:1271–1281.
17. Cunningham VJ, Rabiner EA, Slifstein M, Laruelle M, Gunn RN. Measuring drug occupancy in the absence of a reference region: the Lassen plot re-visited. *J Cereb Blood Flow Metab.* 2010;30:46–50.
18. De Vos H, Convents A, De Keyser J, et al. Autoradiographic distribution of alpha 2 adrenoceptors, NAIBS, and 5-HT1A receptors in human brain using [^{3}H]idazoxan and [^{3}H]rauwolscine. *Brain Res.* 1991;566:13–20.
19. Paterson LM, Tyacke RJ, Robinson ES, Nutt DJ, Hudson AL. In vitro and in vivo effect of BU99006 (5-isothiocyanato-2-benzofuranyl-2-imidazoline) on I2 binding in relation to MAO: evidence for two distinct I2 binding sites. *Neuropharmacology.* 2007;52:395–404.
20. Bonivento D, Milczek EM, McDonald GR, et al. Potentiation of ligand binding through cooperative effects in monoamine oxidase B. *J Biol Chem.* 2010;285:36849–36856.